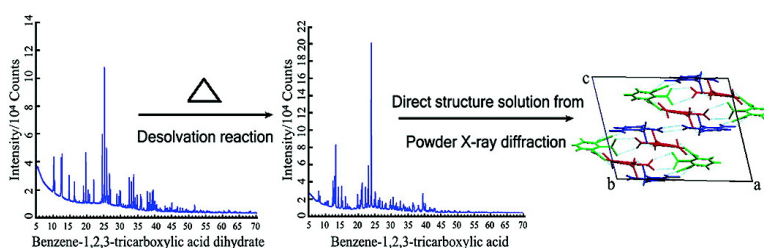


## Structural Understanding of a Molecular Material that Is Accessed Only by a Solid-State Desolvation Process: The Scope of Modern Powder X-ray Diffraction Techniques

Fang Guo, and Kenneth D. M. Harris

*J. Am. Chem. Soc.*, **2005**, 127 (20), 7314-7315 • DOI: 10.1021/ja050733p • Publication Date (Web): 29 April 2005

Downloaded from <http://pubs.acs.org> on March 25, 2009



### More About This Article

Additional resources and features associated with this article are available within the HTML version:

- Supporting Information
- Links to the 5 articles that cite this article, as of the time of this article download
- Access to high resolution figures
- Links to articles and content related to this article
- Copyright permission to reproduce figures and/or text from this article

[View the Full Text HTML](#)



## Structural Understanding of a Molecular Material that Is Accessed Only by a Solid-State Desolvation Process: The Scope of Modern Powder X-ray Diffraction Techniques

Fang Guo and Kenneth D. M. Harris\*

School of Chemistry, Cardiff University, Park Place, Cardiff CF10 3AT, Wales

Received February 4, 2005; E-mail: HarrisKDM@cardiff.ac.uk

There is currently considerable interest in understanding the factors that control the structures of organic molecular crystals, particularly as such structural rationalization is an essential prerequisite for the design of molecular crystals with specific desired properties, an area of activity often called crystal engineering.<sup>1</sup> In general, however, the crystal structure (or structures) observed for a given molecule arises from the interplay of several factors, and rather than attempting to establish generalizations from individual structures taken in isolation, a more informative approach toward the empirical rationalization of crystal structures is to explore structural trends within systematically well-defined families of molecules. Among families of direct interest<sup>2</sup> in this regard are the carboxylic acid derivatives of benzene,  $C_6(CO_2H)_nH_{6-n}$  ( $n = 1-6$ ), of which there are 12 members (including different isomers for some values of  $n$ ). Given the well-established hydrogen-bonding capability of the carboxylic acid groups in molecules within this family<sup>2</sup> and the geometrically well-defined positioning of these groups around the rigid molecular core, general concepts derived from structural rationalization of these materials clearly have wider relevance, for example, in the development of strategies for crystal engineering. Indeed, one member (benzene-1,3,5-tricarboxylic acid; trimesic acid) of this family has received attention<sup>3</sup> with regard to its potential for utilization in crystal design strategies. The structures of most members of this family have been reported previously<sup>4</sup> from single-crystal X-ray diffraction studies, although one member of the family for which the structure has so far remained undetermined is benzene-1,2,3-tricarboxylic acid (BTCA; hemimellitic acid). Although this compound has been of interest from several viewpoints for over 100 years,<sup>5</sup> the crystal structure of BTCA has never been reported. However, a range of solvate structures of BTCA are known, including a dihydrate structure<sup>6</sup> and solvate structures containing several different alcohols<sup>7a</sup> and other solvent molecules.<sup>7a,b</sup> It is clear that crystal growth of a “pure” (nonsolvate) crystal phase of BTCA is rendered difficult by the competitive formation of solvate phases during crystal growth from solution.

For materials of this type that cannot be prepared as a pure (nonsolvate) phase by conventional crystal growth processes,<sup>8</sup> it may be possible to obtain the pure phase of interest by means of a solid-state desolvation process,<sup>9</sup> usually at elevated temperature and/or reduced pressure. Such processes, however, are commonly associated with loss of crystal integrity, such that each single crystal of the parent (solvate) structure yields a polycrystalline aggregate upon desolvation.<sup>10</sup> Single-crystal X-ray diffraction is, therefore, inappropriate for structure determination of the desolvated phase, and alternative approaches for structural characterization are required. Fortunately, in this regard, there have been significant advances in recent years in the opportunities for carrying out complete structure determination of molecular solids directly from powder X-ray diffraction (PXRD) data,<sup>11</sup> particularly through the development of the “direct-space” strategy for structure solution.<sup>11a</sup>

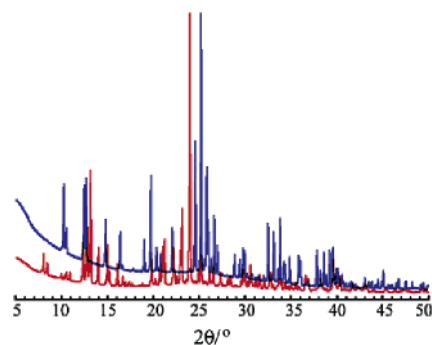


**Figure 1.** PXRD patterns of BTCA dihydrate (blue) and the material obtained following the dehydration process (red).

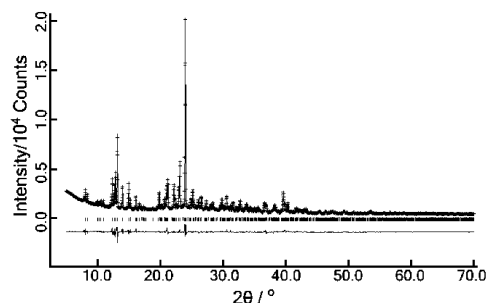


**Figure 2.** Experimental (+ marks), calculated (solid line), and difference (lower line) PXRD profiles for the final Rietveld refinement of BTCA.

The emergence of these techniques now provides a viable route for structural characterization of microcrystalline powder samples produced directly by solid-state processes of the type discussed above. In this paper, we demonstrate the utility of modern PXRD techniques for obtaining structural understanding of molecular materials that can be obtained only by solid-state desolvation processes, focusing on the specific example of BTCA.

In the present work, a polycrystalline sample of pure BTCA was obtained by dehydration of BTCA dihydrate at elevated temperature.<sup>12</sup> PXRD confirmed that this process leads to a new solid phase (Figure 1), with no detectable amount of BTCA dihydrate remaining, and high-resolution solid-state <sup>13</sup>C NMR was consistent with the assignment of the new phase as pure BTCA (with no evidence that any chemical transformation had occurred). Structure determination of the pure phase of BTCA was carried out directly from PXRD data<sup>13,14</sup> using the direct-space genetic algorithm (GA) technique<sup>15</sup> (in the program EAGER<sup>16</sup>) for structure solution,<sup>17</sup> followed by Rietveld refinement<sup>18</sup> using the program GSAS.<sup>19</sup> The good agreement between calculated and experimental PXRD patterns in the final Rietveld refinement (Figure 2) vindicates the correctness of the structure. As there are three independent molecules in the asymmetric unit,<sup>14</sup> each with three unknown torsion angles, this structure represents a comparatively challenging case for direct-space structure solution, and the total number of structural

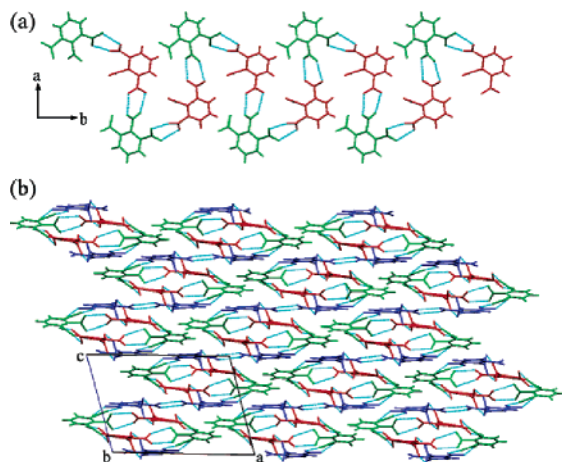


**Figure 3.** Crystal structure of BTCA.<sup>20</sup> The three independent molecules are displayed in different colors (A, green; B, blue; C, red): (a) the hydrogen-bonded chain of A and C molecules viewed approximately along the *c*-axis; (b) the complete crystal structure viewed along the *b*-axis (the AC chains run into the page, with adjacent AC chains cross-linked by hydrogen bonding to B molecules to form two-dimensional slabs that are oriented diagonally (top-right to bottom-left) in the view shown).

variables involved in the optimization is the largest so far reported using the GA technique.

In the structure of BTCA (Figure 3), all carboxylic acid groups participate in intermolecular hydrogen bonding to other carboxylic acid groups via the  $R_2^2(8)$  motif that is often found in carboxylic acid “dimers”. The three independent molecules have similar conformations<sup>20</sup> (the “inner” carboxylic acid group is nearly perpendicular to the ring; the two “outer” carboxylic acid groups lie closer to the plane of the ring). The BTCA structure comprises a number of distinct hydrogen-bonded arrays,<sup>20</sup> which differ substantially from those in BTCA dihydrate, implying that substantial structural reorganization is involved during the solid-state dehydration process. Under such circumstances, loss of crystal integrity during the dehydration process to produce a polycrystalline product phase is not at all surprising.

BTCA is representative of the significant number of materials that cannot be obtained as a nonsolvate structure by conventional solution-state crystallization procedures but can, instead, be accessed directly by a solid-state desolvation process. As such processes invariably lead to the formation of polycrystalline powders, techniques that allow the crystal structures of molecular solids to be determined directly from PXRD data have a key role to play in the structural characterization of new phases produced in this way.

**Acknowledgment.** We are grateful to Cardiff University and Universities UK for a studentship (to F.G.), and to Dr. Mingcan Xu for help with solid-state NMR.

**Supporting Information Available:** Structural data. This material is available free of charge via the Internet at <http://pubs.acs.org>.

## References

- (1) Schmidt, G. M. J. *Pure Appl. Chem.* **1971**, *27*, 647. (b) Thomas, J. M. *Philos. Trans. Royal Soc.* **1974**, *277*, 251. (c) Adams, J. M.; Pritchard, R. G.; Thomas, J. M. *J. Chem. Soc., Chem. Commun.* **1976**, 358. (d) Desiraju, G. R. *Crystal Engineering*; Elsevier: Amsterdam, 1989.
- (2) Leiserowitz, L. *Acta Crystallogr.* **1976**, *B32*, 775.
- (3) (a) Herbstein, F. H. In *Comprehensive Supramolecular Chemistry*; MacNicol, D. D., Toda, F., Bishop, R., Eds.; Pergamon: New York, 1996; Vol. 6, pp 61–83. (b) Melendez, R. E.; Hamilton, A. D. *Top. Curr. Chem.* **1998**, *198*, 97.
- (4) From a survey of Cambridge Structural Database, version 5.26, Nov 2004.
- (5) Agafonov, V. *Compt. Rend.* **1931**, *192*, 99 (which also cites earlier work dated 1897; *Compt. Rend.* **1897**, *124*, 855).
- (6) (a) Takusagawa, F.; Shimada, A. *Bull. Chem. Soc. Jpn.* **1973**, *46*, 2998. (b) Mo, F.; Adman, E. *Acta Crystallogr.* **1975**, *B31*, 192.
- (7) (a) Dale, S. H.; Elsegood, M. R. J.; Coombs, A. E. L. *CrystEngComm* **2004**, *6*, 328. (b) Dale, S. H.; Elsegood, M. R. J. *Acta Crystallogr.* **2004**, *C60*, 444.
- (8) Of course, we cannot rule out the possibility that crystal growth conditions may exist that would favor the formation of the nonsolvate phase, but we refer here to those cases in which all reported attempts to prepare crystals have so far produced only solvate structures.
- (9) Providing that conditions of temperature and pressure exist under which the solid undergoes complete loss of solvent molecules without the molecule of interest undergoing chemical degradation.
- (10) An exception arises for some tunnel solvate structures, for which it may be possible to expel the solvent (guest) molecules with the host tunnel remaining structurally intact; a single crystal of the tunnel solvate would then yield a single crystal of the nonsolvate structure upon desolvation.
- (11) (a) Harris, K. D. M.; Tremayne, M.; Lightfoot, P.; Bruce, P. G. *J. Am. Chem. Soc.* **1994**, *116*, 3543. (b) Harris, K. D. M.; Tremayne, M.; Kariuki, B. M. *Angew. Chem., Int. Ed.* **2001**, *40*, 1626. (c) Harris, K. D. M.; Cheung, E. Y. *Chem. Soc. Rev.* **2004**, *33*, 526. (d) Baerlocher, C.; McCusker, L. B. *Z. Kristallogr.* **2004**, *216* (issue 12), 782–901.
- (12) BTCA dihydrate was prepared by slow evaporation (over 5 days) of water from an aqueous solution of BTCA at ambient temperature. Dehydration was carried out by placing a polycrystalline sample of BTCA dihydrate in an oven at 100 °C for 3.5 h. Previous DTA and TGA studies indicate that these conditions give rise to complete dehydration of BTCA dihydrate (see: Fornies-Marquina, J. M.; Melendez, F.; Chanh, N. B. *J. Therm. Anal.* **1975**, *7*, 263).
- (13) A high quality PXRD pattern of BTCA was recorded at ambient temperature in transmission mode on a Bruker D8 diffractometer [capillary (0.7 mm); Cu K $\alpha$ 1 (Ge-monochromated); linear position-sensitive detector covering 12° in  $2\theta$ ;  $2\theta$  range 5–70°; step size 0.017°; data collection time 12 h]. The high-resolution solid-state <sup>13</sup>C NMR spectrum of BTCA is consistent with the crystal structure having more than one molecule in the asymmetric unit.
- (14) The PXRD pattern of BTCA was indexed using the program DICVOL (Boultif, A.; Louër, D. *J. Appl. Crystallogr.* **1991**, *24*, 987), giving the monoclinic unit cell  $a = 16.85 \text{ \AA}$ ,  $b = 13.75 \text{ \AA}$ ,  $c = 12.03 \text{ \AA}$ ,  $\beta = 105.95^\circ$ . The space group was assigned from systematic absences as  $P2_1/n$ . Unit cell and profile refinement, carried out using the LeBail fitting procedure, led to excellent fit ( $R_{wp} = 5.42\%$ ) for this unit cell and space group. With three independent molecules of BTCA in the asymmetric unit, and  $Z = 4$  for space group  $P2_1/n$ , there are 12 molecules of BTCA in the unit cell; the corresponding density ( $1.56 \text{ g cm}^{-3}$ ) is consistent with typical densities of organic materials.
- (15) (a) Kariuki, B. M.; Serrano-González, H.; Johnston, R. L.; Harris, K. D. M. *Chem. Phys. Lett.* **1997**, *280*, 189. (b) Harris, K. D. M.; Johnston, R. L.; Kariuki, B. M. *Acta Crystallogr.* **1998**, *A54*, 632. (c) Habershon, S.; Harris, K. D. M.; Johnston, R. L. *J. Comput. Chem.* **2003**, *24*, 1766.
- (16) Habershon, S.; Turner, G. W.; Kariuki, B. M.; Cheung, E. Y.; Hanson, A.; Tedesco, E.; Albesa-Jové, D.; Chao, M. H.; Lanning, O. J.; Johnston, R. L.; Harris, K. D. M. *EAGER*; Cardiff University and University of Birmingham, 2004.
- (17) The GA structure solution calculation involved three independent BTCA molecules in the asymmetric unit, representing a total of 27 structural variables (9 variables  $\{x, y, z, \alpha, \beta, \gamma, \tau_1, \tau_2, \tau_3\}$  are required to define the position, orientation, and conformation of each molecule). The GA calculation involved the evolution of 80 generations for a population of 100 structures, with 25 mating operations and 12 mutation operations carried out per generation. The best structure solution was taken as the starting structural model for Rietveld refinement.
- (18) Final Rietveld refinement:  $a = 16.7624(6) \text{ \AA}$ ,  $b = 13.6917(6) \text{ \AA}$ ,  $c = 11.9969(4) \text{ \AA}$ ,  $\beta = 106.0053(25)^\circ$ ,  $R_{wp} = 5.49\%$ ,  $R_p = 4.03\%$ ; 3824 profile points; 180 refined variables.
- (19) Larson, A. C.; Von Dreele, R. B. *GSAS*; Los Alamos Laboratory Report No. LA-UR-86-748, 1987.
- (20) The torsion angles  $\tau_1$  (outer),  $\tau_2$  (inner), and  $\tau_3$  (outer) in the three independent molecules (denoted A, B, and C) are: A (33.7°, 67.7°, 25.0°); B (4.0°, 85.3°, 18.6°); C (37.2°, 69.8°, 32.8°). In the structure, a chain of alternating molecules of types A and C runs along the *b*-axis (Figure 3a). In this chain, each A molecule subtends an angle of 60° and each C molecule subtends an angle of 120°, and there are two A and two C molecules in the repeat unit. The chain appears in projection to have a zigzag architecture, although the chain is not flat and is better described as a “squashed” spiral. The other carboxylic acid group (not involved in the AC chain) of each A and C molecule is hydrogen bonded to a B molecule, such that adjacent A and C molecules along the chain are linked to the same B molecule, giving a cyclic array of three molecules (A, B, and C). Within this cyclic array, each molecule uses one “outer” carboxylic acid group and the “inner” carboxylic acid group, and thus the angle at each node is 60°. Thus, molecules of type B are attached to the periphery of each AC chain by means of these ABC cyclic arrays. Each B molecule has one remaining carboxylic acid group, which forms an  $R_2^2(8)$  linkage to a B molecule that is attached to the periphery of an adjacent AC chain. These B···B interactions provide a cross-linking between adjacent AC chains, and the arrangement of cross-linked AC chains extends as a two-dimensional slab through the crystal (parallel to the (101) plane; Figure 3b). All hydrogen bonding occurs within a slab of this type, and there is no hydrogen bonding between adjacent slabs. Adjacent slabs interact through van der Waals interactions (note the complementary shapes of the surfaces of adjacent slabs).

JA050733P